sciendo

Polish Journal of Chemical Technology, 23, 2, 73—80, 10.2478/pjct-2021-0020

Fe-modified activated carbon obtained from biomass as a catalyst for α-pinene autoxidation

Adrianna Kamińska, Nikola Maciejewska, Piotr Miądlicki, Karolina Kiełbasa*, Joanna Sreńscek-Nazzal, Beata Michalkiewicz

West Pomeranian University of Technology in Szczecin, Faculty of Chemical Technology and Engineering, Engineering of Catalytic and Sorbent Materials Department, Pułaskiego 10, PL 70-322 Szczecin, Poland
**Corresponding author: e-mail: karolina.kielbasa@zut.edu.pl*

The presented work describes the autoxidation of alpha-pinene for the first time using a catalyst based on activated carbon from biomass with introduced Fe. The raw material for the preparation of the carbon material was waste orange peel, which was activated with a KOH solution. The following instrumental methods characterized the obtained catalyst (Fe/O_AC):N_2 adsorption at 77 K, XRD, UV, SEM, TEM, X-ray microanalysis, and catalytic studies. It was shown that the Fe/O_AC catalyst was very active in the autoxidation of alpha-pinene. The main reaction products were: alpha-pinene oxide, verbenone, verbenol, and campholenic aldehyde.

Keywords: activated carbon, carbonaceous catalysts, autoxidation, alpha-pinene, iron particles, biomass.

INTRODUCTION

The preparation of carbon materials from inexpensive and widely available precursors, such as waste biomass from the food industry, has become the main topic of interest in new material research[1–3]. The development of a method of synthesizing carbon materials from biomass enables the use and management of waste, the disposal of which and environmentally safe storage for it has been problematic[4].

Productions of many different carbonaceous materials have been developed e.g. carbon spheres[5, 6], hierarchical porous carbon nanosheets[7], exfoliated graphitic carbon nitride[8], TiO_2-loaded carbon fiber cloths[9], hybrid carbon-TiO_2 spheres[10], TiO_2-reduced graphene oxide[11, 12], carbon nanotubes[13, 14], nano carbon black[13], activated carbon[15–19]. Carbonaceous materials have found a multifunctional application in the fields of catalysis[20–28], photocatalysis[8, 9, 12, 29], water treatment[11], supercapacitors[7], energy storage[30], electrochemical sensor[13], sorption[5, 16, 18, 19, 31] and so on.

The cultivation of citrus trees is considered to be the most developing agricultural sector in recent years. The citrus fruit grown on the most significant scale is the sweet orange (Citrus sinensis), which accounts for up to 70% of citrus fruits' total production and consumption[32]. These fruits are processed on an industrial scale into juices, jams, and marmalades[33]. It is estimated that the citrus fruit processing industry generates nearly 40 tons of waste annually, a significant proportion (~65%) of orange peels[34]. The high content of organic matter in the orange peel makes it challenging to dispose of it quickly because it affects the bacterial flora of the soil. The storage of such waste requires neutralizing the acidic pH of this biomass[35]. The demand for fresh orange juices and citrus preserves is constantly growing, so it is so important to minimize waste during production. Converting waste biomass to carbonaceous materials helps lower the production costs of activated carbons and is a potentially more economical alternative to available commercial carbons[36]. However, before turning waste orange peels into carbonaceous materials, they can be used to extract a very valuable terpene compound: limonene. Limonene itself and its oxidation as well isomerization products have many applications in organic synthesis and the cosmetics, food, perfumery, and cosmetics industries[37–43].

The preparation of activated carbons from orange peels on a laboratory scale is of interest to many researchers. Chen et al.[44] described the preparation of activated carbons from orange peels by pyrolysis at various temperatures and with limited oxygen supply. The carbons obtained in this way can be used as adsorbents for removing toxic compounds from the environment, e.g., naphthalene and 1-naphthol. Giraldo et al.[45] reported the preparation of catalysts prepared by coating with a layer of TiO_2 activated carbon obtained from orange peel. In the biomass impregnation cell, KOH was used as a chemical activator, and the pyrolysis of the carbonaceous substrate was carried out in a vertical tubular reactor at 550°C. The resulting material was then coated with titanium dioxide and used in the NO_X decomposition. Dhorabe[46] described the synthesis of activated carbons from orange peels, which was a waste product from a local marketplace. The researchers used orthophosphoric acid as a chemical activator and then heated the impregnated biomass in a muffle furnace at 350°C. Another team of scientists described the pyrolysis of orange peel in a carbon dioxide environment[47]. Biomass pyrolysis was carried out in a tubular reactor, the flow of N_2 and CO_2 was 300 ml/min, and the temperature range was from 200°C to 700°C. Hui Pan et al.[48] reported the preparation of sulfonated carbons from fresh orange peels by partial hydrothermal carbonization. Concentrated sulfuric acid(VI) was used for chemical activation. The materials obtained in this way were active in the esterification of oleic and citric acids.

Alpha-pinene is a cyclic compound from the group of monoterpenes. This compound can be obtained from turpentine obtained from pine tree resin[49]. Alpha- pinene occurs in nature as a mixture of two enantiomers, the content of which in the mixture may vary depending on the species, age of the tree, and the tissue from which it was obtained (e.g., a needle or xylem)[50, 51]. This compound is used extensively in the perfumery, cosmetics, food, and pharmaceutical industries[52]. This compound is used extensively in the perfumery, cosmetics, food, and pharmaceutical industries. In addition to industrial applications, this compound also exhibits anti-inflammatory,

antibacterial, antiseptic[53], and anti-cancer properties[54]. Alpha-pinene has also been used as a valuable substrate in organic syntheses (oxidation (including autoxidation) and isomerization reactions)[49, 55–60].

There are two ways of conducting the alpha-pinene autoxidation process: autoxidation without the presence of catalysts[61] or with the use of catalysts[62]. In the first step, the reactions were carried out at 100°C using oxygen and without the presence of light. The main products of this reaction were oxygen derivatives such as alpha-foam, verbenone, and myrtenal[61]. The autoxidation of alpha-pinene, which required the use of catalysts, was carried out in the temperature range of 65–90°C. Metal-modified catalysts (Cr, Co, Cu) were used in the reaction. The main products that were obtained during this reaction were alpha-pinene oxide, verbenol, and verbenone[62].

Currently, conducting catalytic reactions in the presence of catalysts is at the center of interest of scientists dealing with catalytic processes. $CoCl_2$ in the presence of oxygen, acetic acid, and acetonitrile as a solvent was used to carry out the catalytic autoxidation of alpha-pinene. The main products were alpha-pinene oxide, alpha-campfolaldehyde, and verbenol and transverbenol. The highest selectivity was recorded for alpha-pinene oxide, and it was 31%, and transverbenol 21%, and also for verbenone 26%. 55% alpha-pinene conversion was achieved[63]. In another work, Mao et al.[64] used the $Fe(III)/SiO_2$ composite as the catalyst. The reaction was carried out in the presence of pure oxygen and using acetonitrile as the solvent. The main products were α-pinene oxide (selectivity was 21%), verbenol (selectivity 45%), and verbenone (selectivity 18%), and the α-pinene conversion was 73%. Gomes et al.[65] carried out alpha-pinene autoxygenation reactions using a $Co(OAc)_2$/bromide catalyst. The main reaction products were cis-verbenyl, verbenone, and myrtenal. The selectivities of the main products were 30%, 20%, and 10% respectively. Wróblewska[49] carried out autoxidation of alpha-pinene on TS-1 catalysts with different Ti content. The main products of autoxidation were alpha-pinene oxide, verbenone, and verbenol. It was found that under the most favorable reaction conditions (80°C, catalyst content 1 wt.%, reaction time 24 h) for the TS-1 20:1 catalyst, the selectivity of alpha-pinene oxide was 30.25 mol%, and the conversion of alpha-pinene reached 41.81 mol%.

The aim of the work is research on the autoxidation of alpha-pinene on Fe/O_AC catalyst. According to the current knowledge, catalyst based on activated carbon obtained from biomass doped with Fe has not been described for this. It has not been used in the process of alpha-pinene autoxidation. The work presented by us illustrates the possibility of utilizing waste such as orange peels from food processing to produce activated carbons. Then, the synthesis of the catalyst based on activated carbon and the use of the catalyst obtained in this way in the catalytic autoxidation of alpha-pinene.

EXPERIMENTAL METHODS

Preparation of activated carbon

The pulp residues were removed from the harvested orange peels and then air-dried at room temperature for 24 hours. Then the material was placed in a dryer at 70°C for 24 hours. The dried biomass was grounded and chemical activated with saturated KOH solution for 3 hours at ambient temperature. The carbon substrate was then dried for 19 hours at 200°C and carbonized at 800°C for 1 hour under a nitrogen flow of 18 l/h. After the carbonization process, the carbon sample was rinsed with distilled water until the filtrate reached neutral pH. Then it was flooded with 1M hydrochloric acid and left for 19 hours. The sample was rinsed again with distilled water until the filtrate pH was approx. 7. The carbon material thus obtained was dried for 19 hours at a temperature of 200°C. The obtained activated carbon was designated as O_AC.

Preparation Fe/O_AC

To apply the iron particles on the carbon surface, 1 g of activated carbon (O_AC) was weighed and suspended in 400 ml of iron salt solution (7.8 g $FeCl_3$ x $6H_2O$ and 3.8 g $FeSO_4x7H_2O$) and then placed on a magnetic stirrer. Then the carbon solution was heated on a magnetic stirrer (700 rpm) to 80°C and kept at this temperature for 90 minutes. After this time, 5M NaOH solution was added dropwise to the material until the pH was about 11, and then it was left on a magnetic stirrer at 80°C, 700 rpm for 1 hour. After impregnation was completed, the sample was removed from the magnetic stirrer and left in the flask for 24 hours at ambient temperature. The material was poured with distilled water until the filtrate pH was constant – about 7. After the filtrate was neutral, the excess water was evaporated from the sample by heating it on an electric cooker. Then the material was dried in an oven at 100°C for 24 hours. The obtained catalyst was designated Fe / O_AC

Alpha-pinene autoxidation

The reaction of alpha-pinene autoxidation was carried out in a glass reactor with a capacity of 5 cm^3, equipped with a reflux condenser and a stirrer. The flask was placed in an oil bath set on a magnetic stirrer with a heating function. 2 g of alpha-pinene (98%, Aldrich) was used for the autoxidation studies. The catalyst activity was tested under the following conditions: the reaction temperature range was 70–120°C, the amount of the catalyst was 0.5–5 wt.%. Samples were taken after 2 hours and 24 hours. The most favorable conditions were determined

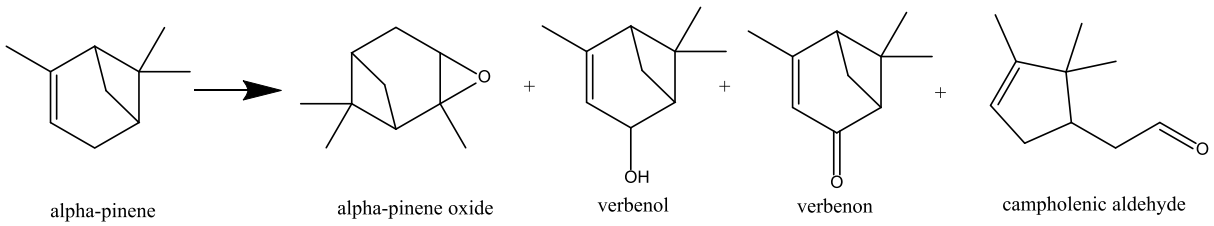

Figure 1. Main products of alpha-pinene autoxidation

based on the conversion and selectivity of alpha-pinene oxide. Other products determined during the tests were: verbenone, verbenol, and campholenic aldehyde (Fig. 1).

To perform the quantitative analysis, the reaction mixture was centrifuged and dissolved in acetone in a weight ratio of 1:10. The quantitative analysis was performed with a Thermo Electron FOCUS chromatograph equipped with an FID detector and a ZB-1701 column (30m x 0.53mm x 1um). The operating parameters of the chromatograph were as follows: helium flow 1.2 ml/min, injector temperature 220°C, detector temperature 250°C, furnace temperature isothermally for 2 minutes at 50°C, increase at a rate of 6°C/min to 120°C, at 120°C isothermally for 4 min, then rising at 15°C/min to 240°C. To determine the composition of post-reaction mixtures, the method of internal normalization was used.

Characterization

For textural characterization was used ASAP Sorption Surface Area and Pore SizeAnalyzer. Nitrogen adsorption isotherm was measured at –196°C. Before adsorption measurements sample was outgassed at 250°C for 19 hours. The specific surface area was calculated using the Brunauer–Emmett–Teller (S_{BET}) equation from nitrogen adsorption isotherms. The total pore volume (V_{tot}) was evaluated from the nitrogen volume adsorbed at a relative pressure of ~0.98. The volumes of micropores were calculated by the DFT method based on nitrogen adsorption. The pore size distribution ($V_{mic(N2)}$) was obtained from the DFT model in the ASAP 2460 Version 3.01 software package based on the N_2 sorption isotherm. DFT used: N_2 at 77 K on carbon (slit N_2-DFT Model adsorption).

The morphology of the sample was observed via scanning electron microscopy with cold emission (UHR FE-SEM Hitachi SU8020). The sample preparation for SEM involved the sprinkling of the powder sample on a double-sided carbon tape mounted on the SEM stub. Images were taken with a 5 kV accelerating voltage using a triple detector system.

The morphology of the sample in greater detail was examined using high-resolution transmission electron microscopy (HR-TEM, Tecnai F20). The catalyst was mounted on a copper grid.

The infrared spectra were acquired at room temperature with a Nicolet 380 ATR-FTIR spectrometer (Thermo Scientific, USA). Sixteen scans were averaged for each sample in the range of 4000–400 cm^{-1}.

The X-ray diffraction (XRD) patterns of the catalyst were recorded by an Empyrean PANalytical X-ray diffractometer using Cu K (λ = 0.154 nm) as the radiation source in the 2θ range 10–80° with a step size of 0.026.

RESULTS AND DISCUSSION

Characteristics of the catalyst

The analysis of nitrogen adsorption-desorption allows determining parameters of the carbon catalyst's porous structure: specific surface area, total pore volume, and micropores. The tested catalyst has surface area values of 452 m^2/g and a total pore volume of 0.496 cm^3/g. The micropore volume estimated based on N_2 adsorption was 0.139 cm^3/g. Fe content in the tested material was at the level of 26.67%. The above results show that it was possible to obtain a carbon catalyst with a relatively high specific surface area with simultaneous high metal content in the catalyst.

Figure 2 shows the adsorption-desorption isotherm for the Fe/O_AC catalyst. In the UPAC classification, the isotherm corresponds to Type-II. Except for the pressure range p/p0 =0.2–0.8, in which it is approximately parallel to the x-axis, which makes it similar in this pressure range to the Type-I isotherm and proves a very small share of mesopores. The isotherm in this section is similar to the Type-I isotherm. Very weak adsorption can be seen here, up to the relative pressure p/po of 0.8. With such high pressures, the macropores are filled. Quantachrome Instruments is not used to measure macropores, but it can be concluded that the pore diameter corresponding to p/p0 ≅ 1 is 784 nm. The visible hysteresis loop is defined as the H3 type, which suggests that there are slotted pores.

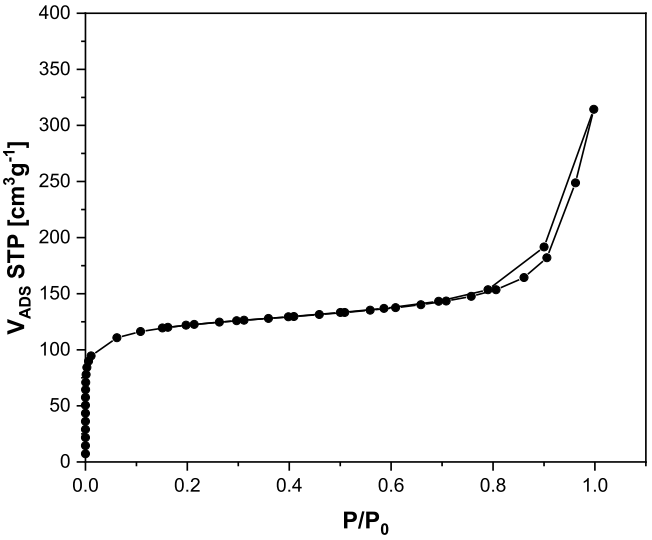

Figure 2. N_2 adsorption-desorption isotherm at –196°C for the obtained Fe/O_AC catalyst

Figure 3 shows the pore size distribution (PSD) of the Fe/O_AC catalyst, determined by the DFT method based on N_2 adsorption at –196°C. Based on Fig. 3, the presence of micropores and the absence of mesopores can be found, which is consistent with the conclusions drawn based on Fig. 2. The DFT method allows the calculation of the pore size up to 100 nm. Taking into account that the maximum pore diameter determined by this method is 784 nm, it can be concluded that only macropores larger than 100 nm are present in the sample. Based on Fig. 2, Fig. 3, and the values of textural parameters, it can be concluded that macropores dominate in the sample. There are also micropores and the proportion of mesopores is negligible. It is also possible to estimate the macropore volume up to a diameter of 784 nm by subtracting V_{mic} from V_{tot}. Approximate macropore volume up to 784 nm is 0.357 cm^3/g.

According to JCPDS card 88-0315 (cubic, Fd-3m) and 79-0416 (cubic, F-43m), the XRD plot showed characteristic peaks of magnetite. Characteristic diffraction peaks of magnetite can be observed at 2θ of 18.32°, 21.26°, 30.32°, 35.65°, 43.30°, 53.87°, 57.33°, 62.87°, 71.50°,

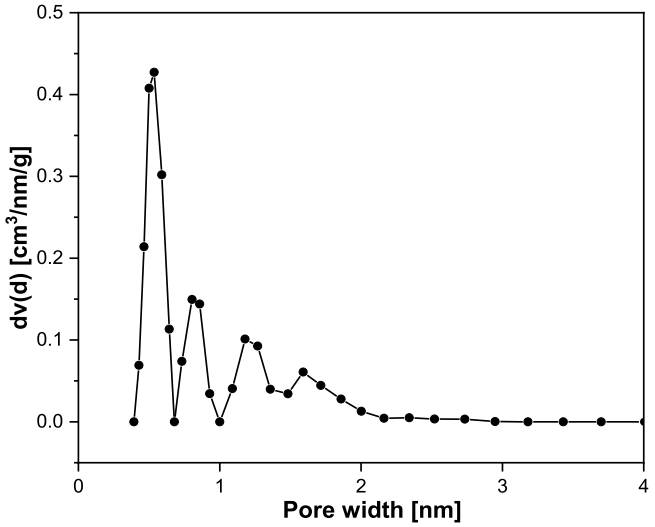

Figure 3. Pore size distribution for Fe/O_AC catalyst

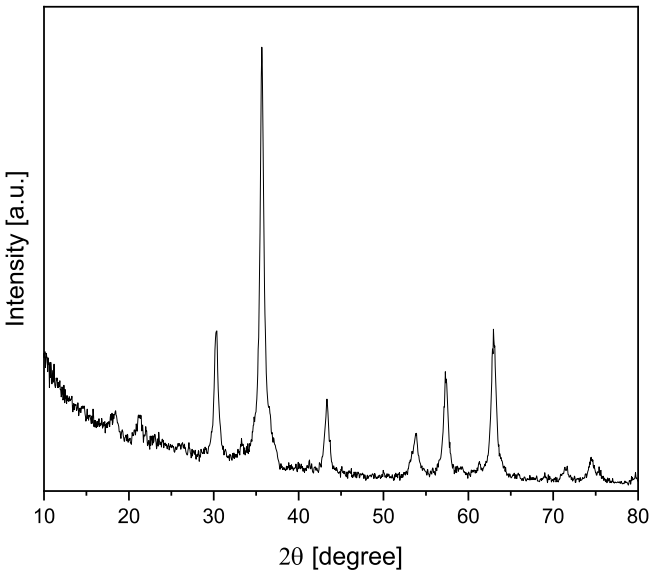

Figure 4. Diffractogram of the obtained catalyst

74.38°. Based on the location and the shape (bordering and intensity) of the peaks, the two first brother signals were identified as magnetite JCPDS card 79-0416. The rest of the signals were assigned to magnetite JCPDS card 88-0315. As all the observed peaks were assigned to the magnetite phase, no peaks for the potential hematite phase could be seen.

The SEM micrographs of Fe/O-AC are shown in Figure 5. SEM images give an idea about the structure and shape of the material. Activated carbon has was a smooth, plated structure with slits (Fig. 5a). At magnification equal to 400 000 Fe_3O_4, nanoparticles on the activated carbon surface were seen. The size of the nanoparticles was about 10–20 nm.

The detailed morphology and structure of the nanoparticles were further investigated by TEM (Fig. 7). The Fe_3O_4 nanoparticles had a semispherical shape with an average size of 18 nm.

Figure 6 shows the EDX spectrum of Fe/O_AC. The sample contained only carbon and iron. The origin of a very small and bright signal about 1.5 keV is aluminum stubs.

The FTIR spectrum of Fe/O_AC catalyst is shown in Figure 8. The characteristic band at 1628 cm^{-1} and wi-

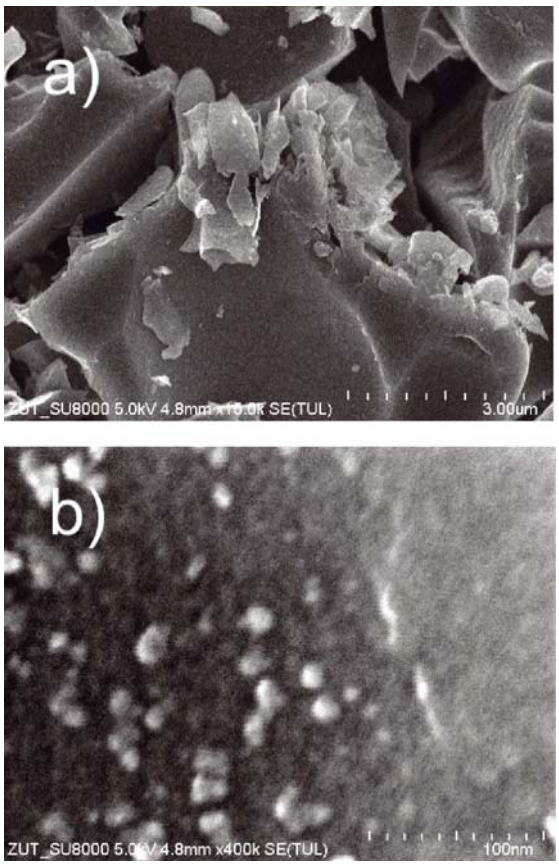

Figure 5. SEM micrographs of the Fe/O_AC

deband between 3000 and 3750 cm^{-1} is attributed to the adsorbed water's existence. In specific, the broad bands (3000–3750 cm^{-1}) can be assigned to OH– stretching vibration mode of adsorbed water and the bending vibration of H_2O is observed at 1628 cm^{-1}. The appearance of two well-defined peaks between 440 and 640 cm^{-1} is due to iron–oxygen (Fe-O), which confirmed that the synthesized nanoparticles are iron oxide[66].

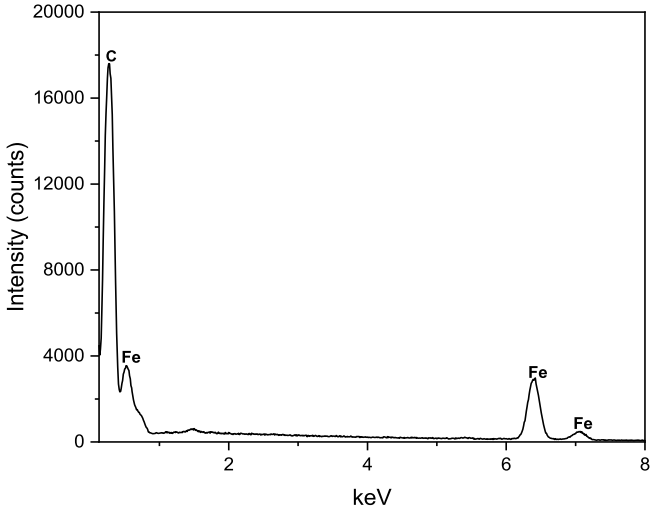

Figure 6. The EDX spectrum of Fe/O_AC

The alpha-pinene autoxidation

In the first stage of research on the Fe/O_AC catalyst activity, the influence of temperature on the course of alpha-pinene autoxidation was checked. The reaction parameters were as follows: temperature in the range of 70–120°C, amount of catalyst 1 wt.%. in relation to alpha-pinene, reaction time 2 and 24 hours. Figure 9

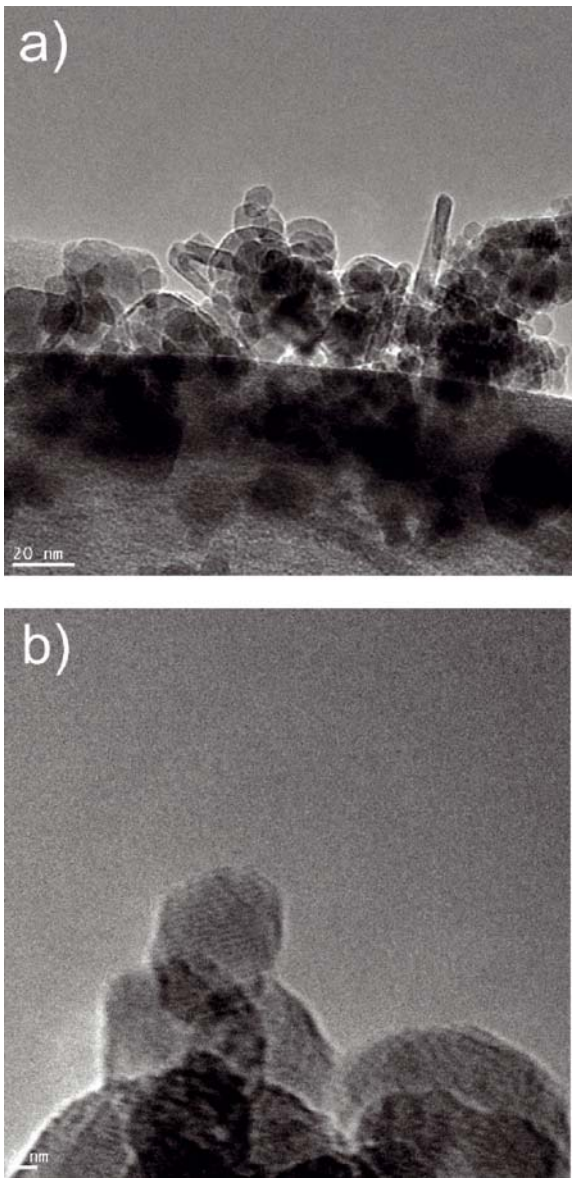

Figure 7. Bright field TEM images of the Fe/O_AC

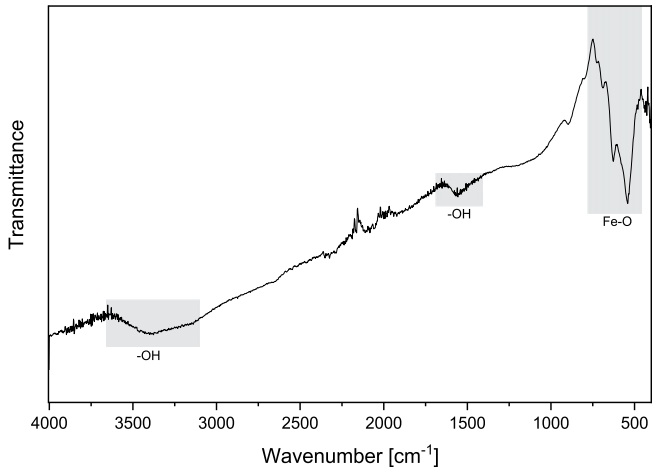

Figure 8. FTIR spectrum of Fe/O_AC catalyst

and Figure 10 show the effect of temperature on alpha-pinene autoxidation. The highest conversion of alpha-pinene (37.5 mol%) was obtained after 24h at 90°C. Above, and below this temperature, the alpha-pinene conversion is lower. The selectivity of alpha-pinene oxide decreases with the progress of the reaction, from 25–30 mol% after 2 hours to 0–15 mol% after 24 hours.

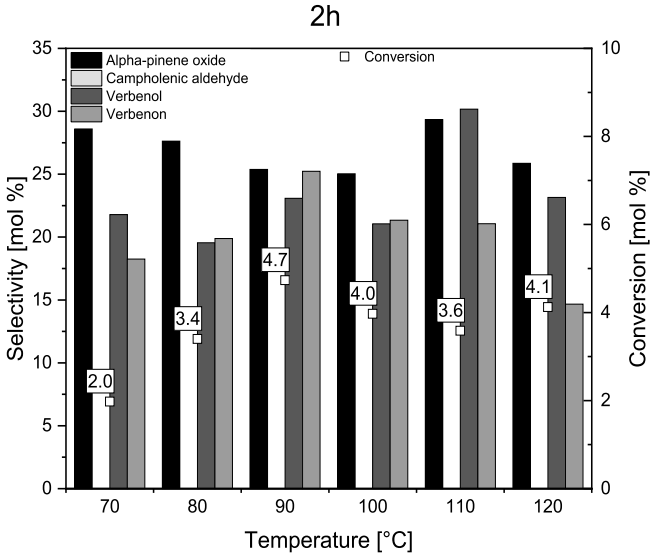

Figure 9. Comparison of the selectivity of the main products and the conversion of alpha-pinene at different temperatures after 2 hours for the Fe/O_AC catalyst

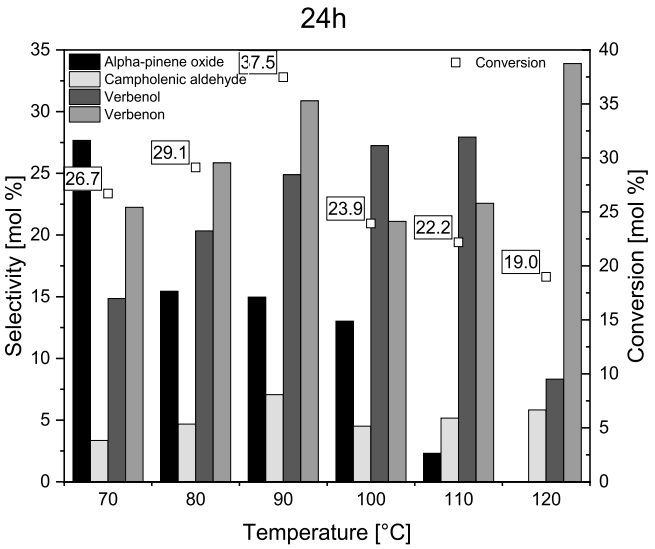

Figure 10. Comparison of the selectivity of the main products and the conversion of alpha-pinene at different temperatures after 24 hours for the Fe/O_AC catalyst

This is due to post-reactions where alpha-pinene oxide reacts to form campholenic aldehyde. As the reaction progresses, the selectivity of verbenol and verbenone also increases. Above 110°C, after 24 hours, a significant decrease in the selectivity of verbenol and the lack of alpha-pinene oxide in the post-reaction mixture can be noticed; it is related to the dimerization and polymerization reactions that take place at higher temperatures. The most preferred reaction temperature is 90°C due to the highest conversion of alpha-pinene in the studied temperature range.

The studies on the effect of the catalyst amount are presented in Figure 11 and Figure 12. The highest alpha-pinene conversion value (37.5 mol%) for the alpha-pinene oxide selectivity (14.9 mol%) was obtained after 24 hours with the catalyst amount of 1 wt.%. For higher catalyst contents in the post-reaction mixture, a significant decrease in the selectivity of alpha-pinene oxide and a decrease in conversion can be noticed. This is due to the very low amount of oxygen in the reaction mixture, resulting in subsequent reactions taking place

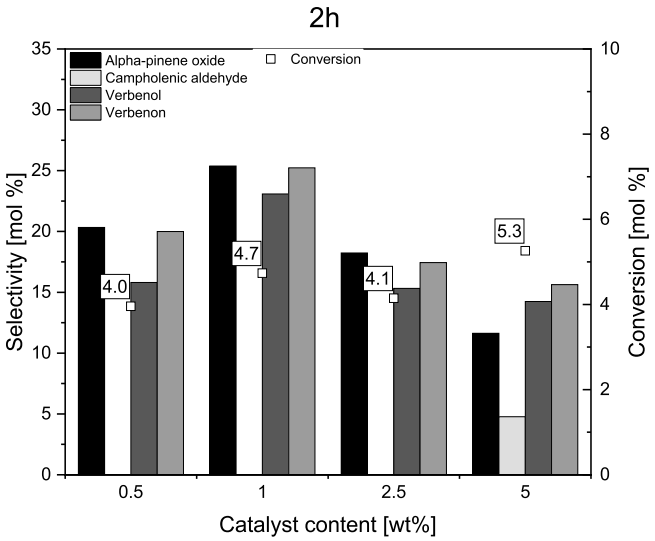

Figure 11. Comparison of the selectivity of the main products and alpha-pinene conversion for different Fe/O_AC catalyst contents [wt.%] after 2 hours

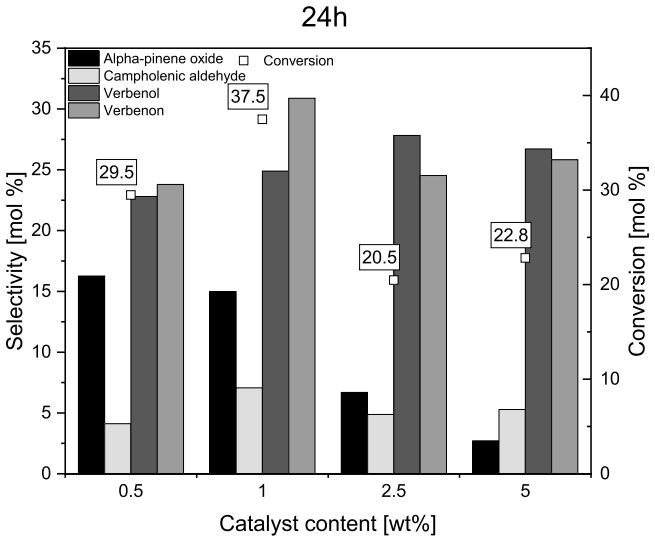

Figure 12. Comparison of the selectivity of the main products and alpha-pinene conversion for different Fe/O_AC catalyst contents [wt.%] after 24 hours

in the presence of the catalyst in the absence of an adequate amount of oxidant. Taking into account the conversion of alpha-pinene and the selectivity of alpha--pinene oxide after 24 hours, the most preferred catalyst content is 1 wt.%.

CONCLUSIONS

The paper presents an ecological method of processing waste such as orange peels into activated carbon and then the use of the material obtained in this way for the synthesis of a Fe-doped carbon catalyst. A relatively high specific surface characterizes the obtained catalyst with a Fe content of 26.67 wt.% and the presence of micropores. The research showed that the obtained Fe/O_AC catalyst was an active catalyst for alpha-pinene autoxidation. The main products of this reaction were: alpha-pinene oxide, verbenone, verbenol, and campfolenic aldehyde. These compounds are used in the perfumery and cosmetics industry due to their fragrance properties. The catalyst allowed to obtain the conversion of 37.5 mol% and selectivity to the alpha-pinene oxide of 14.9 mol% under the most favorable reaction conditions (temperature 90°C, catalyst content in the reaction mixture 1 wt.%, reaction time 24 hours).

LITERATURE CITED

1. Kadirvelu, K. & Namasivayam, C. (2003). Activated carbon from coconut coirpith as metal adsorbent: Adsorption of Cd(II) from aqueous solution. *Adv. Environ. Res.*, 7, 471–478. DOI: 10.1016/S1093-0191(02)00018-7.

2. Xu, C., Hu, Z., Wang, X., Wang, C., Huang, D. & Qian, Y. (2021). Facile preparation of hierarchical porous carbon from orange peels for high-performance supercapacitor. *Int. J. Electrochem. Sci.*, 16, 1–9. DOI: 10.20964/2021.03.07.

3. Serafin, J., Narkiewicz, U., Morawski, A.W., Wróbel, R.J. & Michalkiewicz, B. (2017). Highly microporous activated carbons from biomass for CO2 capture and effective micropores at different conditions. *J. CO2 Util*., 18, 73–79. DOI: 10.1016/j.jcou.2017.01.006.

4. Martin, M.J., Artola, A., Balaguer, M.D. & Rigola, M. (2003). Activated carbons developed from surplus sewage sludge for the removal of dyes from dilute aqueous solutions. *Chem. Eng. J*., 94, 231–239. DOI: 10.1016/S1385-8947(03)00054-8.

5. Staciwa, P., Narkiewicz, U., Sibera, D., Moszyński, D., Wróbel, R.J. & Cormia, R.D. (2019). Carbon Spheres as CO_2 Sorbents. *Appl. Sci.*, 9(16), 3349. DOI: 10.3390/app9163349.

6. Zielinska, B., Michalkiewicz, B., Chen, X., Mijowska, E. & Kaleńczuk, R.J. (2016). Pd supported ordered mesoporous hollow carbon spheres (OMHCS) for hydrogen storage. *Chem. Phys. Lett.,* 647, 14–19. DOI: 10.1016/j.cplett.2016.01.036.

7. Chen, X., Dymerska, A., Mijowska, E., Wen, X., Wróbel, R. (2020). One-step synergistic effect to produce two-dimensional N-doped hierarchical porous carbon nanosheets for high-performance flexible supercapacitors. *ACS Appl. Energy Mater.,* 3, 8562–8572. DOI: 10.1021/acsaem.0c01183.

8. Baca, M., Rychtowski, P., Wróbel, R., Mijowska, E., Kaleńczuk, R. & Zielińska, B. (2020). Surface properties tuning of exfoliated graphitic carbon nitride for multiple photocatalytic performance. *Sol. Energy*, 207, 528–538. DOI: 10.1016/j.solener.2020.07.006.

9. Kusiak-Nejman, E., Czyżewski, A., Wanag,A., Dubicki, M., Sadłowski, M., Wróbel, R.J. & Morawski, A.W. (2020). Photocatalytic oxidation of nitric oxide over AgNPs/TiO_2-loaded carbon fiber cloths. *J. Environ. Manage*., 262, 110343. DOI: 10.1016/j.jenvman.2020.110343.

10. Kusiak-Nejman, E., Mijowska, E., Szymańska, K., Wróbel, R., Wanag, A., Kapica-Kozar, J. & Morawski, W. (2019). Hybrid carbon-TiO_2 spheres: Investigation of structure, morphology and spectroscopic studies. *Appl. Surf. Sci*., 469, 684–690. DOI: 10.1016/j.apsusc.2018.11.093.

11. Wanag, A., Rokicka, P., Kusiak-Nejman, E., Kapica-Kozar, J., Wrobel, R.J., Markowska-Szczupak, A. & Morawski, A.W. (2018). Antibacterial properties of TiO_2 modified with reduced graphene oxide. *Ecotoxicol. Environ. Saf*., 147, 788–793. DOI: 10.1016/j.ecoenv.2017.09.039.

12. Morawski, A.W., Kusiak-Nejman, E., Wanag, A., Kapica-Kozar, J., Wróbel, R.J., Ohtani, B., Aksienionek, M. & Lipińska, L. (2017). Photocatalytic degradation of acetic acid in the presence of visible light-active TiO_2-reduced graphene oxide photocatalysts. *Catal. Today*, 280, 108–113. DOI: 10.1016/j.cattod.2016.05.055.

13. Ziebro, J., Lukasiewicz, I., Grzmil, B., Borowiak-Palen, E. & Michalkiewicz, B. (2009). Synthesis of nickel nanocapsules and carbon nanotubes via methane CVD. *J. Alloys Comp.,* 485, 695–700. DOI: 10.1016/j.jallcom.2009.06.039.

14. Czech, Z., Kowalczyk, A., Pełech, R., Wróbel, R., Shao, L., Bai, Y. & Świderska, J. (2012). Using of carbon nanotubes and nano carbon black for electrical conductivity adjustment

of pressure-sensitive adhesives. *Int. J. Adhes. Adhes*., 36, 20–24. DOI: 10.1016/j.ijadhadh.2012.04.004.

15. Zhang, S., Shi, X., Wróbel, R., Chen, X. & Mijowska, E. (2019). Low-cost nitrogen-doped activated carbon prepared bypolyethylenimine (PEI) with a convenient method for supercapacitor application. *Electrochim. Acta* 294, 183–191. DOI: 10.1016/j.electacta.2018.10.111.

16. Mlodzik, J., Srenscek-Nazzal, J., Narkiewicz, U., Morawski, A.W., Wrobel, R.J. & Michalkiewicz, B. (2016). Activated carbons from molasses as CO_2 sorbents. *Acta Phys. Pol. A* 129, 402–404. DOI: 10.12693/APhysPolA.129.402.

17. Serafin, J., Baca, M., Biegun, M., Mijowska, E., Kaleńczuk, R.J., Sreńscek-Nazzal, J. & Michalkiewicz, B. (2019). Direct conversion of biomass to nanoporous activated biocarbons for high CO_2 adsorption and supercapacitor applications. *Appl. Surf. Sci*., 497. DOI: 10.1016/j.apsusc.2019.143722.

18. Sreńscek-Nazzal, J., Narkiewicz, U., Morawski, A.W., Wróbel, R., Gęsikiewicz-Puchalska, A. & Michalkiewicz, B. (2016). Modification of commercial activated carbons for CO_2 adsorption. *Acta Phys. Pol. A* 129, 394–401. DOI: 10.12693/APhysPolA.129.394.

19. Gesikiewicz-Puchalska, A., Zgrzebnicki, M., Michalkiewicz, B., Narkiewicz, U., Morawski, A.W. & Wrobel, R.J. (2017). Improvement of CO_2 uptake of activated carbons by treatment with mineral acids. *Chem. Eng. J*., 309, 159–171. DOI: 10.1016/j.cej.2016.10.005.

20. . Mlodzik, J., Wróblewska, A., Makuch, E., Wróbel, R. J. & Michalkiewicz, B. (2016). Fe/EuroPh catalysts for limonene oxidation to 1,2-epoxylimonene, its diol, carveol, carvone and perillyl alcohol. *Catal. Today*, 268, 111–120. DOI: 10.1016/j.cattod.2015.11.010.

21. Glonek, K., Wróblewska, A., Makuch, E., Ulejczyk, B., Krawczyk, K., Wróbel, Rafal. J., Koren, Z. C. & Michalkiewicz, B. (2017). Oxidation of limonene using activated carbon modified in dielectric barrier discharge plasma. *Appl. Surf. Sci*. 420, 873–881. DOI: 10.1016/j.apsusc.2017.05.136.

22. Lubkowski, K., Arabczyk, W., Grzmil, B., Michalkiewicz, B. & Pattek-Janczyk, A. (2007). Passivation and oxidation of an ammonia iron catalyst. *Appl. Catal.,* A 329, 137–147. DOI: 10.1016/j.apcata.2007.07.006.

23. Wróblewska, A., Makuch, E., Mlodzik, J. & Michalkiewicz, B. (2017). Fe-carbon nanoreactors obtained from molasses as efficient catalysts for limonene oxidation. *Green Process. Synth*., 6, 397–401. DOI: 10.1515/gps-2016-0148.

24. Wróblewska, A., Makuch, E., Mlodzik, J., Koren, Z.C. & Michalkiewicz B. (2017). Fe/Nanoporous Carbon Catalysts Obtained from Molasses for the Limonene Oxidation Process. *Catal. Lett*. 147, 150–160. DOI: 10.1007/s10562-016-1910-7.

25. Lubkowski, K., Arabczyk, W., Grzmil, B., Michalkiewicz, B. & Pattek-Janczyk, A. (2007). Passivation and oxidation of an ammonia iron catalyst. *Appl. Catal. A-General*, 329, 137–147. DOI: 10.1016/j.apcata.2007.07.006.

26. Wróblewska, A., Serafin, J., Gawarecka, A., Miadlicki, P., Urbas, K., Koren, Z.C., Llorca, J. & Michalkiewicz, B. (2020). Carbonaceous catalysts from orange pulp for limonene oxidation. *Carbon Lett.,* 30, 189–198. DOI: 10.1007/s42823-019-00084-2.

27. Michalkiewicz, B. (2006). The kinetics of homogeneous catalytic methane oxidation. *Appl. Catal.,* A 307, 270–274. DOI: 10.1016/j.apcata.2006.04.006.

28. Wróblewska, A., Makuch, E., Mlodzik, J., Koren, Z.C. & Michalkiewicz, B. (2018). Oxidation of limonene over molybdenum dioxide-containing nanoporous carbon catalysts as a simple effective method for the utilization of waste orange peels. *React. Kinet. Mech. Catal*., 125, 843–858. DOI: 10.1007/s11144-018-1468-z.

29. Michalkiewicz, B., Sreńscek-Nazzal, J., Tabero, P., Grzmil, B. & Narkiewicz, U. (2008). Selective methane oxidation to formaldehyde using polymorphic T-, M-, and H-forms of niobium(V) oxide as catalysts. *Chem. Pap*., 62, 106–113. DOI: 10.2478/s11696-007-0086-4.

30. Gong, J., Michalkiewicz, B., Chen, X., Mijowska, E., Liu, J., Jiang, Z., Wen, X. & Tang, T. (2014). Sustainable conversion of mixed plastics into porous carbon nanosheets with high performances in uptake of carbon dioxide and storage of hydrogen. *ACS Sustain. Chem. Eng*., 2, 2837–2844. DOI: 10.1021/sc500 603h.

31. Kapica-Kozar, J., Pirog, E., Kusiak-Nejman, E., Wrobel, R.J., Gesikiewicz-Puchalska, A., Morawski, A.W., Narkiewicz, U. & Michalkiewicz, B. (2017). Titanium dioxide modified with various amines used as sorbents of carbon dioxide. *New J. Chem*., 41, 1549–1557. DOI: 10.1039/c6nj02808j.

32. Okwu, D. & Emenike, I. (2006). Evaluation of the phytonutrients and vitamins content of citrus fruits. *Int. J. Mol. Med. Adv. Sci*., 2(1), 1–6.

33. Simpson, K. (1981). Tropical and subtropical fruits: composition, properties and uses. Ed. S. Nagy and P.E. Shaw. Westport, Conn.: Avi (1980), pp. 570, $US 49.50.

34. Ferguson, J.J. (2004). World Markets for Organic Fresh Citrus and Juice. Edis1–5 (1969). http://edis.ifas.ufl.edu

35. Sharma, K., Mahato, N., Cho, M.H. & Lee, Y.R. (2017). Converting citrus wastes into value-added products: Economic and environmently friendly approaches. *Nutrition*. 34, 29–46. DOI: 10.1016/j.nut.2016.09.006.

36. Dhelipan, M., Arunchander, A., Sahu, A.K. & Kalpana, D. (2017). Activated carbon from orange peels as supercapacitor electrode and catalyst support for oxygen reduction reaction in proton exchange membrane fuel cell. *J. Saudi Chem. Soc*., 21, 487–494. DOI: 10.1016/j.jscs.2016.12.003.

37. Wróblewska, A. (2014). The epoxidation of limonene over the TS-1 and Ti-SBA-15 catalysts. *Molecules*, 19, 19907–19992. DOI: 10.3390/molecules191219907.

38. Wróblewska, A., Makuch, E. & Miądlicki, P. (2016). The studies on the limonene oxidation over the microporous TS-1 catalyst. *Catal. Today*, 268, 121–129. DOI: 10.1016/j.cattod.2015.11.008.

39. Gawarecka, A. & Wróblewska, A. (2018). Limonene oxidation over Ti-MCM-41 and Ti-MWW catalyst with t-butyl hydroperoxide as the oxidant. *Reac. Kinet. Mech. Cat*., 124(2), 523–543. DOI: 10.1007/s11144-018-1401-5.

40. Retajczyk, M. & Wróblewska, A. (2017). The isomerization of limonene over the Ti-SBA-15 catalyst—the influence of reaction time, temperature, and catalyst content. *Catalysts*, 7(9), 273, 1–14. DOI: 10.3390/catal7090273.

41. Retajczyk, M. & Wróblewska, A. (2019). Isomerization and dehydroaromatization of R(+)-limonene over the Ti--MCM-41 catalyst: effect of temperature, reaction time and catalyst content on product yield. *Catalysts*, 9, 508 (1–11). DOI: 10.3390/catal9060508.

42. . Retajczyk, M, Wróblewska, A., Szymańska, A. & Michalkiewicz, B. (2019). Isomerization of limonene over natural zeolite-clinoptilolite. *Clay Miner*. 54, 121–129. DOI: 10.1180/clm.2019.18.

43. Retajczyk, M., Wróblewska, A., Szymańska, A., Miądlicki, P., Koren, Zvi, C. & Michalkiewicz, B. (2020). Synthesis, characterization, and catalytic applications of the Ti-SBA-16 porous material in the selective and green isomerizations of limonene and S-carvone. *Catalysts* 10, 1452. DOI: 10.3390/catal10121452.

44. Chen, B. & Chen, Z. (2009). Sorption of naphthalene and 1-naphthol by biochars of orange peels with different pyrolytic temperatures. *Chemosphere*, 76, 127–133. DOI: 10.1016/j.chemosphere.2009.02.004.

45. Giraldo, L. & Moreno-Pirajan, J.C. (2014). Activated carbon prepared from orange peels coated with titanium oxide nanoparticles: Characterization and applications in the decomposition of NOx. *Orient. J. Chem*., 30, 451–461. DOI: 10.13005/ojc/300207.

46. Dhorabe, P.T., Lataye, D.H. & Ingole, R.S. (2017). Adsorptive removal of 4-nitrophenol from aqueous solution by activated carbon prepared from waste orange peels. *J. Hazard. Toxic. Radioact. Waste.,* 21, 04016015. DOI: 10.1061/(asce) hz.2153-5515.0000332.

47. Kwon, D., Oh, J.I., Lam, S.S., Moon, D.H. & Kwon, E.E. (2019). Orange peel valorization by pyrolysis under the carbon dioxide environment. *Bioresour. Technol*., 285, 121356. DOI: 10.1016/j.biortech.2019.121356.

48. Pan, H., Sun, J., Liu, Y., Zhang, J. & Zhou, S. (2021). Preparation of sulfonated carbon derived from orange peel and its application in esterification. *Chem. Phys. Lett*., 770, 138395. DOI: 10.1016/j.cplett.2021.138395.

49. Wróblewska, A., Tołpa, J., Kłosin, D., Miądlicki, P., Koren, Z.C. & Michalkiewicz, B. (2020). The application of TS-1 materials with different titanium contents as catalysts for the autoxidation of α-pinene. *Microporous Mesoporous Mater.,* 305, 110384. DOI: 10.1016/j.micromeso.2020.110384.

50. Phillips, M.A., Savage, T.J. & Croteau, R. (1999). Monoterpene synthases of loblolly pine (Pinus taeda) produce pinene isomers and enantiomers. *Arch. Biochem. Biophys.* 372, 197–204. DOI: 10.1006/abbi.1999.1467.

51. Sjödin, K., Persson, M., Borg-Karlson, A.K. & Norin, T. (1996). Enantiomeric compositions of monoterpene hydrocarbons in different tissues of four individuals of Pinus sylvestris. *Phytochem*., 41, 439–445. DOI: 10.1016/0031-9422(95)00652-4.

52. Trytek, M., Paduch, R., Fiedurek, J. & Kandefer-Szerszeń, M. (2007). Monoterpeny - Stare związki, nowe zastosowania i biotechnologiczne metody ich otrzymywania. *Biotechnol*., 76, 135–155.

53. Kucharska, M., Szymańska, J.A., Wesołowski, W., Bruchajzer, E. & Frydrych, B. (2018). Porównanie składu chemicznego wybranych olejków eterycznych stosowanych w chorobach układu oddechowego. *Med. Pr*., 69, 167–178. DOI: 10.13075/mp.5893.00673.

54. Donaghy, J. & McKay, A. (1994). Pectin extraction from citrus peel by polygalacturonase produced on whey. *Bioresour. Technol.*, 47, 25–28. DOI: 10.1016/0960-8524(94)90024-8.

55. Wróblewska, A., Miądlicki, P. & Makuch, E. (2016). The isomerization of a-pinene over the Ti-SBA-15 catalyst – the influence of catalyst content and temperature. *Reac. Kinet. Mech. Cat*., 119, 641–654. DOI: 10.1007/s11144-016-1059-9.

56. Wróblewska, A., Miądlicki, P., Sreńscek-Nazzal, J., Sadłowski, M., Koren, Zvi C. & Michalkiewicz, B. (2018). Alpha--pinene isomerization over Ti-SBA-15 catalysts obtained by the direct method: The influence of titanium content, temperature, catalyst amount and reaction time. *Micropor. Mesopor. Mater.,* 258, 72–82. DOI: 10.1016/j.micromeso.2017.09.007.

57. Wróblewska, A., Miądlicki, P., Tołpa, J., Sreńscek-Nazzal, J., Koren, Zvi, C. & Michalkiewicz, B. (2019). Influence of the titanium content in the Ti-MCM-41 catalyst on the course of the alfa-pinene isomerization process. *Catalysts* 9, 396(1–16). DOI: 10.3390/catal9050396.

58. Wróblewska, A., Miądlicki, P. & Makuch, E. (2016). The isomerization of a-pinene over the Ti-SBA-15 catalyst – the influence of catalyst content and temperature. *Reac. Kinet. Mech. Cat.*, 119, 641–654. DOI: 10.1007/s11144-016-1059-9.

59. Wróblewska, A., Miądlicki, P., Sreńscek-Nazzal, J., Sadłowski, M., Koren, Zvi, C. & Michalkiewicz, B. (2018). Alpha--pinene isomerization over Ti-SBA-15 catalysts obtained by the direct method: The influence of titanium content, temperature, catalyst amount and reaction time. *Micropor. Mesopor. Mater*., 258, 72–82. DOI: 10.1016/j.micromeso.2017.09.007.

60. Wróblewska, A., Miądlicki, P., Tołpa, J., Sreńscek-Nazzal, J., Koren, Zvi, C. & Michalkiewicz, B. (2019). Influence of the titanium content in the Ti-MCM-41 catalyst on the course of the alfa-pinene isomerization process. *Catalysts*, 9, 396(1–16). DOI: 10.3390/catal9050396.

61. Moore, R.N., Golumbic, C. & Fisher, G.S. (1956). Autoxidation of α-Pinene. *J. Am. Chem. Soc.,* 78, 1173–1176. DOI: 10.1021/ja01587a022.

62. Rothenberg, G., Yatziv, Y. & Sasson, Y. (1998). Comparative autoxidation of 3-Carene and α-Pinene: Factors governing regioselective hydrogen abstraction reactions. *Tetrahedron,* 54, 593–598. DOI: 10.1016/S0040-4020(97)10319-2.

63. Silva, M.J., Robles-Dutenhefner, P., Menini L. & Gusevskaya, E.V. (2003). Cobalt catalyzed autoxidation of monoterpenes in acetic acid and acetonitrile solutions. *J. Mol. Catal. A:Chem*., 201, 71–77. DOI: 10.1016/S1381-1169(03)00180-8.

64. Mao, J., Hu, X., Li, H., Sun, Y. & Chen, Z. (2008). Iron chloride supported on pyridine-modified mesoporous silica : an efficient and reusable catalyst for the allylic oxidation of olefins with molecular oxygen. *Green. Chem.,* 8. DOI: 10.1039/b807234e.

65. De Fhima, M., Gomes, T. & Antunes, O.A.C. (1997). Autoxidation of limonene , cy-pinene and / 3-pinene by dioxygen catalyzed by Co(OAc2)/ bromide. *J. Mol. Catal. A:Chem.* 121, 2(3), 145–155. DOI: 10.1016/S1381-1169(97)00010-1

66. Hwang, S.W., Umar, A., Dar, G.N., Kim, S.H. & Badran, R.I. (2014). Synthesis and characterization of iron oxide nanoparticles for phenyl hydrazine sensor applications. *Sens. Lett.,* 12(1), 97–101. DOI: 10.1166/sl.2014.3224.